



Cite this: *CrystEngComm*, 2023, 25, 5748

Ligand competition on uranyl ion: further examples of zwitterionic vs. anionic carboxylate coordination†

Sotaro Kusumoto,^a Youssef Atoini,^b Yoshihiro Koide,^a Shinya Hayami,^a Yang Kim,^{*c} Jack Harrowfield^{*d} and Pierre Thuéry^{*e}

Four uranyl ion mixed-ligand complexes involving anionic and zwitterionic carboxylate donors have been synthesized under solvo-hydrothermal conditions. $[(UO_2)_2(pda)_2(bet)_2]$ (1), where pda^{2-} is 1,3-phenylenediacetate and bet is betaine, crystallizes as a monoprotic coordination polymer in which all ligands are κ^2O,O' -chelated and $UO_2(pda)(bet)_2$ units are decorating groups to the $UO_2(pda)$ chain. In $[bcebpH_2][UO_2(bcebp)(H_2O)_2][UO_2(tcenm)]_4 \cdot 2H_2O$ (2), where $tcenm^{3-}$ is tris(2-carboxylatoethyl)nitromethane and bcebp is 4,4'-bis(2-carboxylatoethyl)-4,4'-bipyridinium, the two ligands are separated into different polymeric units, di- (hcb) and monoprotic, respectively, and hydrogen bonding of the $bcebpH_2^{2+}$ counterions to chains results in heteropolycatenation, with the counterions crossing four hexagonal networks. $[(UO_2)_2(pht)_2(bcpcb)]$ (3), where pht^{2-} is phthalate and bcpcb is 1,4-bis(4'-carbonylatopyridiniomethyl)benzene, is a diprotic network with V_2O_5 topology, while $[(UO_2)_4(O)_2(kpim)_2(bcpcb)]$ (4), where $kpim^{2-}$ is 4-ketopimelate, is a diprotic network with bis(μ_3 -oxo)-bridged U_4O_2 secondary building units as nodes and sql topology. In this last case, the large size of the rings allows for $2D + 2D \rightarrow 3D$ inclined polycatenation to occur. The relative strength of anionic and zwitterionic carboxylate donors and the importance of weak interactions in the structures are discussed.

Received 25th August 2023,
Accepted 12th September 2023

DOI: 10.1039/d3ce00845b

rs.li/crystengcomm

Introduction

In exploring the hypothesis that the use of neutral, polyzwitterionic carboxylate-donor ligands might provide an avenue to both cationic coordination polymers and mixed-ligand polymers of higher dimensionality with the uranyl ion,^{1,2} our initial expectations were based upon the seminal work of Mak and co-workers in which it had been demonstrated that the solid state bonding capacities of zwitterionic and anionic carboxylates in their main group and transition metal ion complexes were essentially identical.^{3,4} While this proved to be a useful guide, the actual situation

has proven to be more complicated, particularly in regard to the composition and structure of mixed-ligand carboxylate complexes. In the present work, we provide further illustration of the remarkable variety in this chemistry.

Three different zwitterionic carboxylates have been used (Scheme 1), the simplest being betaine (trimethylammonioacetate, bet), which is involved in only a small number of uranyl ion complexes⁵ reported in the Cambridge Structural Database (CSD, version 5.44),⁶ generally investigated in the context of ionic liquid studies. The second zwitterionic ligand is 4,4'-bis(2-carboxylatoethyl)-4,4'-bipyridinium (bcebp), which has been shown to give mixed-ligand species with the uranyl ion when associated with either isophthalate or 1,2-, 1,3- and 1,4-phenylenediacetates, with these complexes displaying woven, polycatenated or cage-like structures.^{2d} The third ligand is 1,4-bis(4'-carbonylatopyridiniomethyl)benzene (bcpcb) which, associated with the tricarballylate coligand, has been shown to give a complex in which the two ligands are segregated into different polymeric units, one a cationic, six-fold interpenetrated framework, and the other an anionic nanotubular assembly included in the channels defined by the former.^{2e} These ligands have been associated with anionic polycarboxylate coligands, 1,3-phenylenediacetate (pda^{2-}) for bet, tris(2-carboxylatoethyl)nitromethane ($tcenm^{3-}$)

^a Department of Material & Life Chemistry, Kanagawa University, 3-27-1 Rokkakubashi, Kanagawa-ku, Yokohama 221-8686, Japan

^b Technical University of Munich, Campus Straubing, Schulgasse 22, 94315 Straubing, Germany

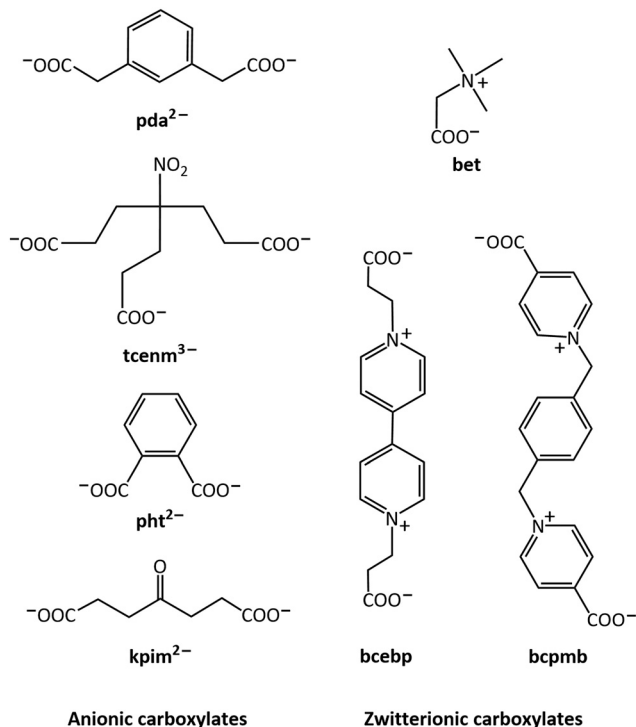
^c Department of Chemistry, Graduate School of Science and Technology, Institute of Industrial Nanomaterials (IINA), Kumamoto University, 2-39-1 Kurokami, Chuo-ku, Kumamoto 860-8555, Japan. E-mail: hayami@kumamoto-u.ac.jp, ykim@kumamoto-u.ac.jp

^d Université de Strasbourg, ISIS, 8 allée Gaspard Monge, 67083 Strasbourg, France. E-mail: harrowfield@unistra.fr

^e Université Paris-Saclay, CEA, CNRS, NIMBE, 91191 Gif-sur-Yvette, France. E-mail: pierre.thuery@cea.fr

† CCDC 2289765–2289768. For crystallographic data in CIF or other electronic format see DOI: <https://doi.org/10.1039/d3ce00845b>





Scheme 1 The anionic and zwitterionic carboxylates used as ligands.

for bcebp, and phthalate (pht²⁻) or 4-ketopimelate (kpim²⁻) for bcpcb. The four resulting complexes, which have been characterized by their crystal structure and their emission spectrum in the solid state, provide further evidence of the versatility of such anionic/zwitterionic carboxylate systems, which makes this approach very promising in the field of uranyl-based coordination polymer studies.⁷

Experimental

Synthesis

Caution! Uranium is a radioactive and chemically toxic element, and uranium-containing samples must be handled with suitable care and protection. Small quantities of reagents and solvents were employed to minimize any potential hazards arising both from the presence of uranium and the use of pressurized vessels for the syntheses.

[UO₂(NO₃)₂(H₂O)₂].4H₂O (RP Normapur, 99%) was purchased from Prolabo. Betaine (bet), 1,3-phenylenediacetic acid (pdaH₂), tris(2-carboxyethyl)nitromethane (tcnmH₃), phthalic acid (phtH₂) and 4-ketopimelic acid (kpimH₂) were from Sigma-Aldrich. 4,4'-Bis(2-hydroxycarbonyl)ethyl-4,4'-bipyridinium dichloride (bcebpH₂Cl₂) and 1,4-bis(4'-hydroxycarbonylpyridiniummethyl)benzene dihexafluorophosphate (bcpcbH₂(PF₆)₂) were synthesized as previously reported.^{2d,e} Elemental analyses were performed by MEDAC Ltd. For all syntheses, the solutions were placed in 10 mL tightly closed glass vessels (Pyrex culture tubes with SVL15 stoppers and Teflon-coated seals, provided by VWR) and heated at 140 °C in a sand bath (Harry Gestigkeit ST72). The crystals were

grown in the hot, pressurized solutions and not as a result of a final return to ambient conditions, as apparent from direct observation.

[(UO₂)₂(pda)₂(bet)₂] (1). Betaine (12 mg, 0.10 mmol), 1,3-phenylenediacetic acid (20 mg, 0.10 mmol), and [UO₂(NO₃)₂(H₂O)₂].4H₂O (50 mg, 0.10 mmol) were dissolved in a mixture of water (0.5 mL) and acetonitrile (0.2 mL). Yellow crystals of complex 1 were obtained within one month (20 mg, 35%). Chemical analysis indicates the presence of about one water molecule in excess of the formula derived from crystal structure determination. Anal. calcd for C₃₀H₃₈N₂O₁₆U₂ + H₂O: C, 30.62; H, 3.43; N, 2.38. Found: C, 30.88; H, 3.40; N, 2.27%.

[bcebpH₂][UO₂(bcebp)(H₂O)₂][UO₂(tcnm)]₄.2H₂O (2). bcebpH₂Cl₂ (19 mg, 0.05 mmol), tcnmH₃ (28 mg, 0.10 mmol), and [UO₂(NO₃)₂(H₂O)₂].4H₂O (50 mg, 0.10 mmol) were dissolved in a mixture of water (0.5 mL) and acetonitrile (0.2 mL). Yellow crystals of complex 2 were obtained within three weeks (14 mg, 22% based on U). Chemical analysis indicates the presence of about four water molecules in excess of the formula derived from crystal structure determination. Anal. calcd for C₇₂H₉₀N₈O₅₄U₅ + 4H₂O: C, 27.08; H, 3.09; N, 3.51. Found: C, 26.60; H, 3.11; N, 3.69%.

[(UO₂)₂(pht)₂(bcpcb)] (3). bcpcbH₂(PF₆)₂ (26 mg, 0.04 mmol), phtH₂ (9 mg, 0.05 mmol), and [UO₂(NO₃)₂(H₂O)₂].4H₂O (25 mg, 0.05 mmol) were dissolved in a mixture of water (0.5 mL) and *N,N*-dimethylacetamide (0.2 mL). A few yellow crystals of complex 3 were obtained within two days.

[(UO₂)₄(O)₂(kpim)₂(bcpcb)] (4). bcpcbH₂(PF₆)₂ (26 mg, 0.04 mmol), kpimH₂ (9 mg, 0.05 mmol), and [UO₂(NO₃)₂(H₂O)₂].4H₂O (25 mg, 0.05 mmol) were dissolved in a mixture of water (0.5 mL) and *N,N*-dimethylacetamide (0.2 mL). Yellow crystals of complex 4 were obtained within three days (11 mg, 49% based on U). Anal. calcd for C₃₄H₃₂N₂O₂₄U₄: C, 22.63; H, 1.79; N, 1.55. Found: C, 22.72; H, 1.90; N, 1.77%.

Crystallography

Data collections were performed at 100(2) K on a Bruker D8 Quest diffractometer using an Incoatec Microfocus Source (I μ S 3.0 Mo) and a PHOTON III area detector, and operated with APEX3.⁸ The data were processed with SAINT,⁹ and empirical absorption corrections were made with SADABS.¹⁰ The structures were solved by intrinsic phasing with SHELXT,¹¹ and refined by full-matrix least-squares on *F*² with SHELXL,¹² using the ShelXle interface.¹³ When possible, the hydrogen atoms bound to oxygen atoms were retrieved from residual electron density maps and they were refined with geometric restraints. All other hydrogen atoms in all the compounds were introduced at calculated positions and treated as riding atoms with an isotropic displacement parameter equal to 1.2 times that of the parent atom (1.5 for CH₃). For compounds 1–3, the SQUEEZE¹⁴ software was used to subtract the contribution of disordered solvent molecules to the structure factors. Crystal data and structure refinement parameters are given in Table 1. Drawings were made with



Table 1 Crystal data and structure refinement details

	1	2	3	4
Chemical formula	C ₃₀ H ₃₈ N ₂ O ₁₆ U ₂	C ₇₂ H ₉₀ N ₈ O ₅₄ U ₅	C ₃₆ H ₂₄ N ₂ O ₁₆ U ₂	C ₃₄ H ₃₂ N ₂ O ₂₄ U ₄
<i>M</i> /g mol ⁻¹	1158.68	3121.66	1216.63	1804.73
Crystal system	Monoclinic	Triclinic	Triclinic	Triclinic
Space group	<i>P</i> 2 ₁ / <i>n</i>	<i>P</i> $\bar{1}$	<i>P</i> $\bar{1}$	<i>P</i> $\bar{1}$
<i>a</i> /Å	19.7847(6)	11.3984(3)	9.7035(6)	11.6695(4)
<i>b</i> /Å	10.1109(3)	11.4010(4)	9.7140(6)	12.5806(5)
<i>c</i> /Å	35.7831(12)	21.9898(9)	10.6933(7)	14.2442(4)
α /°	90	88.8056(15)	79.359(4)	87.1650(13)
β /°	90.6793(16)	79.8563(13)	75.201(3)	88.3831(12)
γ /°	90	60.8371(10)	71.662(3)	84.6902(15)
<i>V</i> /Å ³	7157.6(4)	2449.37(15)	919.03(10)	2079.07(12)
<i>Z</i>	8	1	1	2
Reflections collected	80 597	117 605	22 763	93 483
Independent reflections	13 583	9279	3482	7902
Observed reflections [<i>I</i> > 2σ(<i>I</i>)]	11 497	8406	3277	7573
<i>R</i> _{int}	0.064	0.077	0.060	0.050
Parameters refined	932	676	253	577
<i>R</i> ₁	0.044	0.025	0.030	0.022
<i>wR</i> ₂	0.093	0.052	0.077	0.053
<i>S</i>	1.123	1.049	1.069	1.102
$\Delta\rho_{\min}/e \text{ \AA}^{-3}$	-1.85	-1.74	-0.72	-2.44
$\Delta\rho_{\max}/e \text{ \AA}^{-3}$	2.09	0.94	3.45	1.09

ORTEP-3,¹⁵ and VESTA,¹⁶ and topological analyses were performed with ToposPro.¹⁷ Special details are as follows:

Compound 1. The aromatic ring of one pda²⁻ ligand is disordered over two positions which have been refined as idealized hexagons with occupancy parameters constrained to sum to unity and restraints on displacement parameters. The SQUEEZE software added about 4 electrons per formula unit, possibly corresponding to approximately 0.5 water molecule, a number smaller than that found from chemical analysis (see above).

Compound 2. The two aromatic rings of the central part of the zwitterionic ligand are rotationally disordered, and one complete diaromatic model containing both positions has been refined with an occupancy of 0.5. 2-Component twinning was taken into account. The SQUEEZE software added 73 electrons per formula unit, possibly corresponding to approximately 7 water molecules, a number in excess of that found from chemical analysis (see above), probably due to water loss upon drying.

Luminescence measurements

Emission spectra were recorded on solid samples using an Edinburgh Instruments FS5 spectrofluorimeter equipped with a 150 W CW ozone-free xenon arc lamp, dual-grating excitation and emission monochromators (2.1 nm mm⁻¹ dispersion; 1200 grooves per mm) and an R928P photomultiplier detector. The powdered compounds were pressed to the wall of a quartz tube, and the measurements were performed using the right-angle mode in the SC-05 cassette. An excitation wavelength of 420 nm was used in all cases and the emission was monitored between 450 and 600 nm. The quantum yield measurements were performed by using a Hamamatsu Quantaurus C11347 absolute

photoluminescence quantum yield spectrometer and exciting the samples between 300 and 400 nm (250 and 300 nm for 1).

Results and discussion

Synthesis

Given the lability of the uranyl ion, it is anticipated that complexation equilibria in solvothermal syntheses would be established essentially simultaneously with attainment of the reaction conditions, so that the nature of the product finally isolated must depend on its solubility and/or rate of crystallization. This explains the rather widespread observation that the stoichiometry of the isolated species does not necessarily match that of the reaction mixture that is further exemplified in the present work. The situation can be complicated by independent reactions of cosolvents and possibly by photochemistry of the uranyl ion but in the present cases neither acetonitrile nor *N,N*-dimethylacetamide, both known to undergo hydrolysis under solvothermal conditions, has provided components of the products, though the buffering action of dimethylammonium acetate is possibly the reason for the partial uranyl ion hydrolysis observed in complex 4.

Crystal structures

The ligand betaine is a mono- not a poly-zwitterion but the structure of its mixed anionic-zwitterionic carboxylate complex provides both confirmation of the observations of Mak *et al.*,³ and illustration of the formation of a genuine mixed-ligand species where both ligands are found on one uranyl centre. The asymmetric unit in the complex [(UO₂)₂(pda)₂(bet)₂] (1) contains four independent uranium atoms, all with hexagonal-bipyramidal coordination. U1 and



U2 are in similar environments, being κ^2O,O' -chelated by three carboxylate groups from three pda^{2-} ligands, whereas U3 and U4 are also in similar environments, κ^2O,O' -chelated by one pda^{2-} and two terminating *bet* ligands (Fig. 1). The range of U–O(carboxylate) bond lengths for pda^{2-} -derived chelate units spans that of the *bet* units (Table 2), with the differences between mean bond lengths around the four metal centres not being statistically significant. The only instance in which the difference between the two types of donors would approach significance is that of atoms U3 and U4, with a bond length slightly shorter for anionic than for zwitterionic donors. The bond valence parameters (BV)¹⁸ calculated with PLATON¹⁹ allow an estimation of bond strength as related to bond length. Although they have to be taken with appropriate caution, these values match the trend previously found for another mixed-ligand complex,^{2e} with greater strength of the axial (oxo) component for the zwitterion-bound atoms, and slightly smaller strength for zwitterionic than for anionic donors. Only two metal atoms (U1 and U2) are involved in the formation of the polymer as 3-coordinated (3-c) nodes with two pda^{2-} ligands as edges, while the two $UO_2(pda)(bet)_2$ units are simple decorating groups. As a result, a monoperic polymer only is formed, parallel to [100], built from a central chain with lateral protruding groups giving the whole a sawtooth shape. The polymer chain involving U1 and U2 has a fairly flattened helical form not unlike that of one of the chains found in $[(UO_2)_4(pda)_4Ni_2(tpyc)_4]\cdot CH_3CN\cdot 2H_2O$,^{1a} where *tpyc*⁻ is 2,2':6',2''-terpyridine-4'-carboxylate, here with chains of

opposite chirality lying side-by-side and interdigitated so as to build layers parallel to (001). Small solvent-accessible voids are present and the Kitaigorodsky packing index (KPI, evaluated with PLATON¹⁹) is 0.69 (disorder excluded). With all aromatic ring centroid...centroid distances larger than 4.8 Å, no π -stacking interaction is found.

The complex $[bcebpH_2][UO_2(bcebp)(H_2O)_2][UO_2(tcenm)]_4\cdot 2H_2O$ (2) contains both the protonated zwitterion precursor as a counter-cation and the zwitterion itself as a ligand. Complete separation of the complex subunits formed by the anionic and zwitterionic ligands is found here, as in some previous cases.^{1a,2a,c,e} Atoms U1 and U2 are tris(κ^2O,O')-chelated by three *tcenm*³⁻ ligands, while atom U3, located on an inversion centre, is chelated by two zwitterionic ligands and bound to two additional water molecules (Fig. 2). Here also, although the U–O bond lengths involving *bcebp* are within the range defined by those with *tcenm*³⁻, calculation of BV parameters fits the trend previously found (Table 3). As in complexes where the zwitterion is not present,²⁰ the two independent $UO_2(tcenm)^-$ units, with both the metal and ligand being 3-c nodes, form inequivalent but almost identical, close-to-planar diperic polymer sheets parallel to (001), which have the point symbol $\{6^3\}$ and the **hcb** topological type. The nitro groups project at an angle of near 80° to the mean plane, all being located on the same side of a given sheet. The inequivalence of the diperic sheets arises from the fact that two sheets involving U1 centres lie adjacent with the nitro substituents projecting into the intervening space; on each side of this

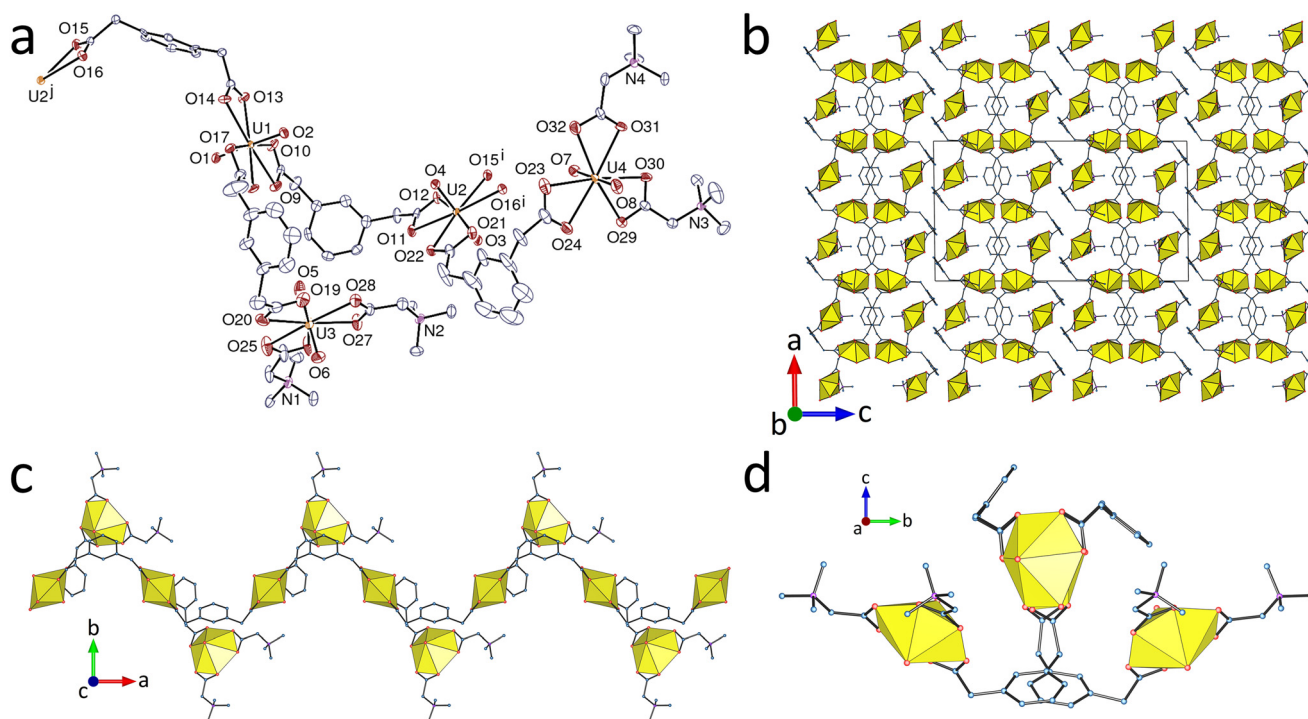


Fig. 1 (a) View of complex 1 with displacement ellipsoids shown at the 50% probability level and hydrogen atoms omitted. Only one component of the disordered part is represented. Symmetry codes: $i = x + 1, y, z$; $j = x - 1, y, z$. (b) Packing with chains viewed side-on showing uranium coordination polyhedra. (c) and (d) Two views of the monoperic assembly.



Table 2 U–O(carboxylate) bond lengths and mean values,^a mean values of bond valence parameters for individual carboxylate oxygen atoms (BV_{carb}) and BV sums (axial and total) in **1**

U ^{VI} centre	Ligand	U–O (Å)	<U–O> (Å)	<BV _{carb} >	BV _{axial} sum	BV _{tot} sum
U1	pda ²⁻	2.482(5)/2.449(6)	2.47(2)	0.440(17)	3.456	6.097
		2.495(5)/2.470(5)				
		2.439(6)/2.485(5)				
U2	pda ²⁻	2.499(5)/2.450(6)	2.47(2)	0.44(2)	3.433	6.087
		2.489(6)/2.451(5)				
		2.481(5)/2.433(6)				
U3	pda ²⁻ bet	2.439(6)/2.452(7)	2.446(6)	0.461(6)	3.588	6.241
		2.479(7)/2.470(6)	2.479(12)	0.433(10)		
		2.498(6)/2.467(6)				
U4	pda ²⁻ bet	2.443(6)/2.450(6)	2.447(3)	0.461(3)	3.521	6.154
		2.475(6)/2.498(6)	2.484(14)	0.428(13)		
		2.465(5)/2.497(6)				

^a As in all following tables, values separated by a slash correspond to the two bond lengths of a chelated carboxylate group, and the estimated standard deviation (esd) on mean bond length values measures the dispersion of individual values and does not take into account the individual esds.

double sheet lies a sheet incorporating U2 where the nitro groups project away from the U1 sheet and towards a third sheet composed of strands of the monoperiodic polymer incorporating U3 lying side by side. This stacking of the sheets in the order U3–U2–U1–U1–U2 repeats down [001] and is complicated by the fact that bcebpH₂²⁺ cations penetrate the sheets at an angle of close to 55° to [001] in such a way as to link consecutive U3 sheets through hydrogen bonding of coordinated water molecules (on U3) to the carboxylic acid groups of bcebpH₂²⁺ [O24⋯O25, 2.801(5) Å; O24–H⋯O25, 154(7)°]. There is also a strong hydrogen bonding interaction of the carboxylic acid proton of each terminus with carboxylate oxygen atoms of the U2 sheets [O25⋯O15, 2.613(4) Å; O25–H⋯O15, 177(5)°], supported by CH(methylene)⋯O(carboxylate) interactions involving both U1 and U2 sheets [C⋯O, 3.202(6) and 3.231(5) Å]. There are presumably hydrogen bonding interactions involving the uncoordinated water molecules but as the water hydrogen atoms were not located, these cannot be defined with certainty. Similarly, partial disorder of the bound bcebp phenyl groups (see Experimental) renders the significance of an approach of nitro groups uncertain and prevents a detailed description of aromatic interactions. Each bcebpH₂²⁺ cation crosses two hexagonal rings pertaining to the two central anionic sheets, and the hydrogen bonds to the coordinated water molecules at both ends cross the hexagonal rings of the outermost anionic sheets, with the carboxylic oxygen atom being very close to the ring. The cations thus link the chains through the intervening space of four anionic layers, and the whole may be seen as a 2D + 2D → 3D hydrogen-bonded heteropolycatenated triperiodic assembly.

The complex [(UO₂)₂(pht)₂(bcpmb)] (**3**) marks a return to a true mixed-ligand species where each U^{VI} centre is bound to both ligands, although the interactions of the two with the metal ion differ rather markedly. Phthalate is a ligand which has been widely studied in its uranyl ion complexes²¹ and while its coordination modes vary considerably, chelation

and multiple bridging interactions are very commonly seen. This is the case in **3**, where the pentagonal-bipyramidal U^{VI} centre has a phthalate ligand bound in a 7-membered chelate ring and is also bound to two other phthalate anions by κ¹O coordination of the carboxylate oxygen atoms not involved in the chelation, and to one oxygen atom from bcpmb (Fig. 3). The large chelate ring appears to limit the interactions of the zwitterion to κ¹O donation rather than the κ²O,O' chelation found in **1** and **2**. As seen in Table 4, this compound gives no hint of a difference between anionic and zwitterionic donors. The metal centre and pht²⁻ are 4- and 3-c nodes, respectively, and bcpmb is a simple edge in the diperiodic network formed parallel to (012̄), which has the {4²·6³·8}{4²·6} point symbol and the V₂O₅ topological type. This topology is quite frequent in uranyl ion coordination polymers involving one large linker, and it has been found in isophthalate complexes^{21j} as well as in several mixed-ligand species involving zwitterionic coligands (and one of them isophthalate also).^{2b,c} One probably significant parallel-displaced π-stacking interaction involves pht²⁻ ligands in adjacent layers [centroid⋯centroid, 3.824(3) Å; dihedral angle, 0°; slippage, 1.14 Å]. The sheets are nearly planar and the packing contains some solvent-accessible voids (KPI, 0.68). It is notable that association of bcpmb with pht²⁻ leads to a very different complex to that found for [NH₄]₂[UO₂(bcpmb)₂][UO₂(tca)]₄·2H₂O, where tca is tricarallylate,^{2e} though one with perhaps more familiar features.

Partial hydrolysis of the uranyl ion is not an unusual feature of solvothermal syntheses of uranyl coordination polymers,⁷ and U^{VI} in [(UO₂)₄(O)₂(kpim)₂(bcpmb)] (**4**) is present as a bis(μ₃-oxo)-bridged U₄O₂ cluster to which both kpim²⁻ and bcpmb are bound through μ₂-κ²O,O':κ¹O chelating-bridging and μ₂-κ¹O:κ¹O' bridging for the former, and κ²O,O' chelating for the latter (Fig. 4). The asymmetric unit contains two independent but similar complex units, each with two uranium atoms, all in somewhat irregular pentagonal-bipyramidal environments, and the U₄O₂



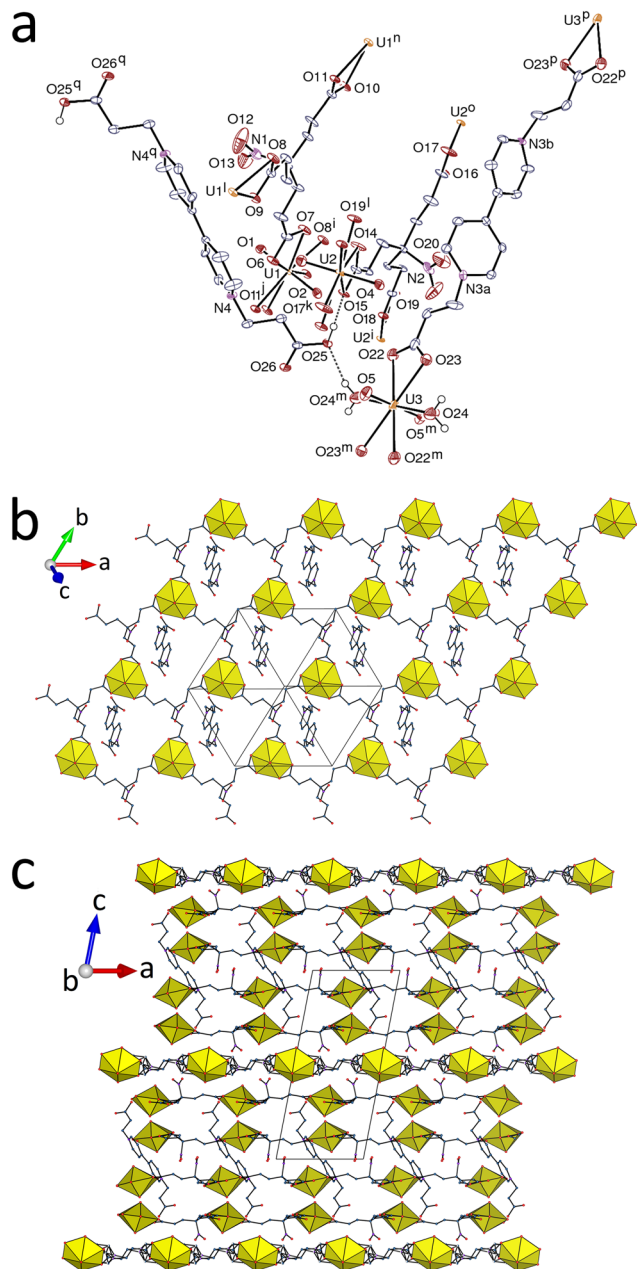


Fig. 2 (a) View of complex 2 with displacement ellipsoids shown at the 50% probability level. Solvent molecules and carbon-bound hydrogen atoms are omitted, and hydrogen bonds are shown as dashed lines. Only one component of the disordered part is represented. Symmetry codes: $i = x, y - 1, z$; $j = x + 1, y - 1, z$; $k = x + 1, y, z$; $l = x, y + 1, z$; $m = 2 - x, -y, 1 - z$; $n = x - 1, y + 1, z$; $o = x - 1, y, z$; $p = -x, 1 - y, 1 - z$; $q = 1 - x, 1 - y, 2 - z$. (b) View of one diperiodic subunit and the included bcebpH₂²⁺ cations. (c) Packing with layers viewed edge-on.

secondary building units (SBUs) are of the common type (i) in the classification of Loiseau *et al.*^{7c} The U–O bond lengths and bond valence parameters are given in Table 5: atoms U1 and U3 show most clearly the trend previously found, with bond lengths significantly (for U1 at least) larger, and in consequence bond valence parameters smaller, for zwitterionic than for anionic donors. The bond lengths for

U2 and U4, only bound to kpim²⁻ and oxo bridges, display a very large dispersion due to the very large values associated with the chelating (and bridging) carboxylate groups (the mean value for chelating carboxylate groups on pentagonal-bipyramidal uranium centres from the CSD is 2.47(4) Å). However, here also, the bond valence parameter of axial donors is larger for the zwitterion-bound metal ions. The mean U–O(μ_3 -oxo) bond length over all metal centres is 2.26(3) Å, in agreement with the value of 2.26(6) Å from the CSD, and the mean bond valence parameter is 0.66(4), larger than for any carboxylate donor, as expected (the BV sums for these groups are 2.015 and 1.958, thus confirming their oxo, and not hydroxo, nature); the planarity around the μ_3 -oxo bridges is shown by the sum of the three U–O–U angles being 358.6 and 360.0° for O16 and O24, respectively. In that both ligands are bound to the cluster, it can be considered as a “true” mixed-ligand species, although only kpim²⁻ interacts with both inequivalent metal ions. While only one other uranyl ion complex of kpim²⁻ has been structurally characterized,^{2b} the ligand appears to have some resemblance to tcnm³⁻ in that the central functionality is not involved in uranyl ion coordination in either of the now known structures. The flexibility of kpim²⁻ is apparent in conformations where the carboxylate donors are essentially divergent in the known species^{2b} and more convergent in the two inequivalent but very similar presently defined forms. Considering only the interactions of kpim²⁻ with the tetranuclear SBU, the full structure can be dissected into two inequivalent but closely similar, double-stranded, monoprotic polymer chains running along [100]. These chains are linked through bridging by the dizwitterions to form diperiodic networks which have the $\{4^4 \cdot 6^2\}$ point symbol and **sql** topological type, with however a double kpim²⁻ edge (simple [(U₄O₂)(kpim)]₂ ring). The sheets containing U1 and U2 lie parallel to (010) while those containing U3 and U4 lie parallel to (001), meaning that the different sheets are near orthogonal (~87.2°). The rings having bcpmb as edges are sufficiently large (~8 × 9 Å in the central part) to allow for 2D + 2D → 3D inclined polycatenation with [100] as the zone axis to occur (Fig. 5). This and other large dizwitterions have previously been shown to give entangled structures with the uranyl ion, when associated with anionic coligands.^{1c,2b,c,d,e,22}

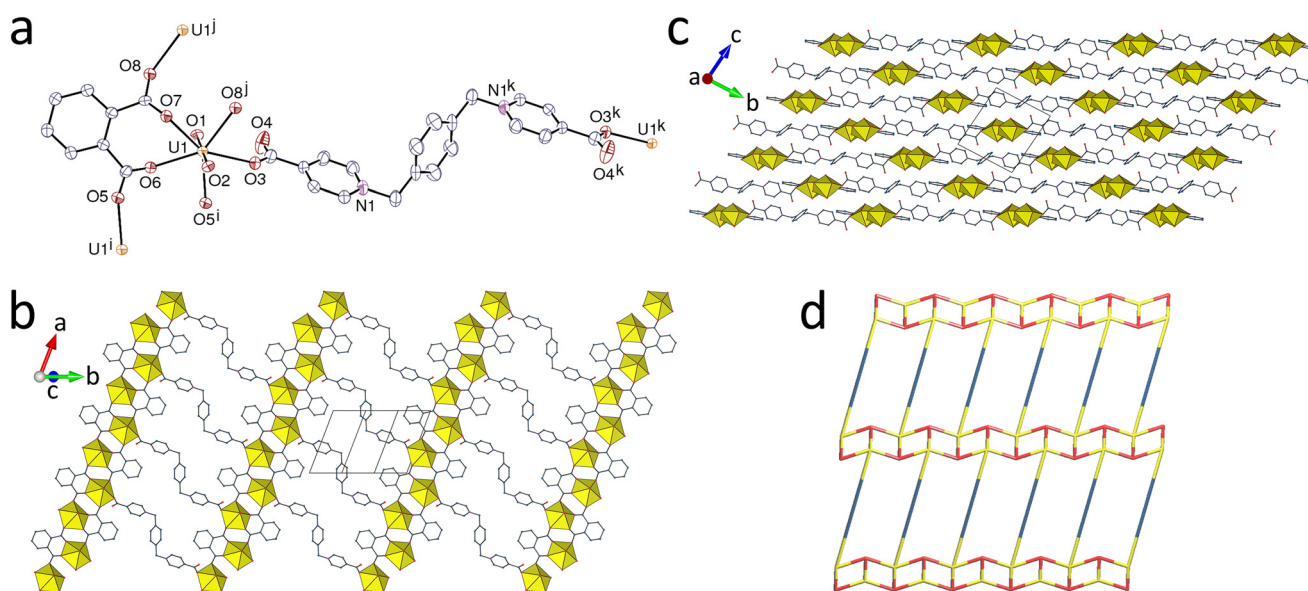
It is also notable that, while entangled uranyl-based coordination polymers have frequently been reported lately, those containing large polynuclear SBUs as nodes remain quite unusual.^{2c,23} The central regions of the zwitterions project upon one another where the different sheets cross each other, in such a way that terminal rings of two zwitterions involving N2 sandwich the central ring of another involving N1, implying significant parallel-displaced π -stacking interactions [centroid⋯centroid, 3.817(3) Å; dihedral angle, 10.1(2)°; slippage, 1.27 Å] (Fig. 6). As expected for such an intricate structure, there is no solvent-accessible void (KPI, 0.72).

While bond valence values of the present complexes offer some evidence for differences in the bonding capacity



Table 3 U–O(carboxylate) bond lengths and mean values, mean value of bond valence parameters for individual carboxylate oxygen atoms (BV_{carb}) and BV sums (axial and total) in **2**

U^{VI} centre	Ligand	U–O (Å)	$\langle U-O \rangle$ (Å)	$\langle BV_{\text{carb}} \rangle$	BV_{axial} sum	BV_{tot} sum
U1	tcenm ³⁻	2.430(3)/2.503(3)	2.46(3)	0.45(2)	3.463	6.138
		2.440(3)/2.473(3)				
		2.455(3)/2.483(3)				
U2	tcenm ³⁻	2.500(3)/2.454(3)	2.46(2)	0.45(2)	3.453	6.147
		2.457(3)/2.434(3)				
		2.483(3)/2.433(3)				
U3	bcebp	2.480(4)/2.496(3)	2.488(8)	0.424(7)	3.539	6.132

**Fig. 3** (a) View of compound **3** with displacement ellipsoids shown at the 50% probability level and hydrogen atoms omitted. Symmetry codes: $i = -x, 1 - y, 1 - z$; $j = 1 - x, 1 - y, 1 - z$; $k = 2 - x, -y - 1, -z$. (b) View of the diperiodic network. (c) Packing with layers viewed edge-on. (d) Nodal representation of the network (yellow, uranium nodes; red, pht²⁻ nodes; blue, bcpcb edges; view down [001] with [100] horizontal).

between anionic and zwitterionic carboxylates, it may be noted that the coordination modes of the zwitterion ligands further exemplify what has been seen generally in our studies, *i.e.* that these are very largely of either κ^1O or κ^2O , O' forms, with bridging modes rather rare and of the form $\mu_2-\kappa^1O:\kappa^1O'$ only, all indicative of a diminished capacity compared to anionic donors. The monodentate κ^1O mode leaves one carboxylate oxygen atom available for interactions other than coordination to U^{VI} , seen in complex **3** to be a $CH\cdots O$ interaction involving a relatively acidic N^+ -methylene group proton [$C\cdots O$, 3.284(8) Å; $C-$

$H\cdots O$, 143°], indicating that any U–O interaction energy gained by rearrangement to a κ^2O,O' form must be less than that of the hydrogen bond. Significantly, in the rather few examples known of uranyl ion complexes of zwitterionic ligands where the charge on nitrogen is due to its protonation, thus providing a rather strong hydrogen bond donor site, the ligand binding mode is exclusively κ^1O .²⁴ The ligand 1,4-bis(iminodiacetatomethyl)-2,3,5,6-tetramethylbenzene,^{24d} for example, behaves as a tetrakis(κ^1O) species where each NH proton only has close contacts (~ 2.1 – 2.3 Å) to the two uncoordinated oxygen

Table 4 U–O(carboxylate) bond lengths and mean values, mean value of bond valence parameters for individual carboxylate oxygen atoms (BV_{carb}) and BV sums (axial and total) in **3**

U^{VI} centre	Ligand	U–O (Å)	$\langle U-O \rangle$ (Å)	$\langle BV_{\text{carb}} \rangle$	BV_{axial} sum	BV_{tot} sum
U1	pht ²⁻	2.360(4)	2.38(2)	0.53(2)	3.409	6.042
		2.354(4)				
		2.390(4)				
		2.402(4)				
	bcpcb	2.387(3)	0.517			



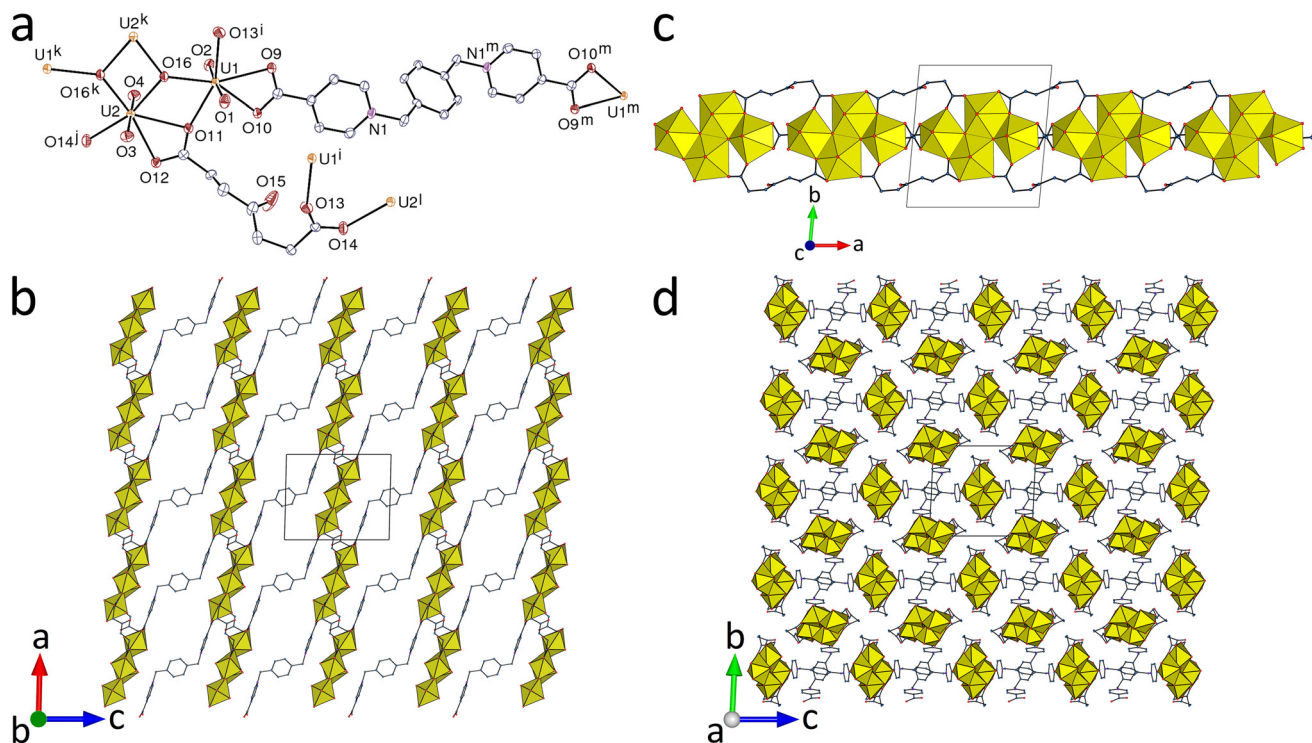


Fig. 4 (a) View of one of the two independent units in compound 4 with displacement ellipsoids shown at the 50% probability level and hydrogen atoms omitted. Symmetry codes: $i = 2 - x, 1 - y, 1 - z$; $j = x - 1, y, z$; $k = 1 - x, 1 - y, 1 - z$; $l = x + 1, y, z$; $m = 3 - x, 1 - y, 2 - z$. (b) and (c) Two views of one individual diperiodic network. (d) View of the polycatenated framework.

Table 5 U–O(carboxylate) bond lengths and mean values, mean value of bond valence parameters for individual carboxylate oxygen atoms (BV_{carb}) and BV sums (axial and total) in 4

U^{VI} centre	Ligand	U–O (Å)	$\langle U-O \rangle$ (Å)	$\langle BV_{\text{carb}} \rangle$	BV_{axial} sum	BV_{tot} sum
U1	kpim ²⁻	2.366(4)	2.35(2)	0.56(2)	3.406	6.063
		2.327(4)				
U2	bcpmb kpim ²⁻	2.487(4)/2.505(4)	2.496(9)	0.418(7)	3.356	5.930
		2.535(4)/2.582(4)				
U3	kpim ²⁻	2.388(4)	2.35(4)	0.56(4)	3.426	6.073
		2.385(4)				
U4	bcpmb kpim ²⁻	2.485(4)/2.473(4)	2.479(6)	0.432(6)	3.353	5.943
		2.548(4)/2.543(4)				
		2.365(4)				

atoms of its iminodiacetate unit, indicative of weak, possibly fluxional, hydrogen bonding even though the N–H \cdots O bond angles ($\sim 110^\circ$) are far from 180° . This interaction is supported by those of O \cdots HO(water) and O \cdots HC, perhaps indicating that it is the sum of these interactions that determines the observations. Indeed, in the structure of the uranyl ion complex of the dizwitterion of DOTA (1,4,7,10-tetraazacyclododecane- N,N',N'',N''' -tetraacetic acid) and oxalate,^{24c} the closest contacts to the NH units are to intra-annular nitrogen atoms, and the uncoordinated carboxylate oxygen atoms are strongly hydrogen bonded to uranyl-coordinated water, so that other than possibly through their influence on the zwitterion conformation, the NH units do not directly affect the carboxylate bonding mode.

Luminescence properties

Complexes 1, 3 and 4, but not 2, are emissive, and their emission spectra measured in the solid state under excitation at 420 nm are shown in Fig. 7. The photoluminescence quantum yields (PLQYs) of 9, 4 and 4% for 1, 3 and 4, respectively, are low to moderately large, as usual for such complexes. It is notable that for the measurement of the PLQY of 1, the sample was excited at a higher energy than the others, *i.e.* in a region in which such complexes absorb more light, due to the tiny amount of sample available (see Experimental). The spectrum of 1 is best resolved and it displays the typical vibronic progression due to the $S_{11} \rightarrow S_{00}$ and $S_{10} \rightarrow S_{0v}$ ($v = 0-4$) transitions of the uranyl ion,²⁵ with the four main maxima at 499, 521, 546 and 573 nm, which



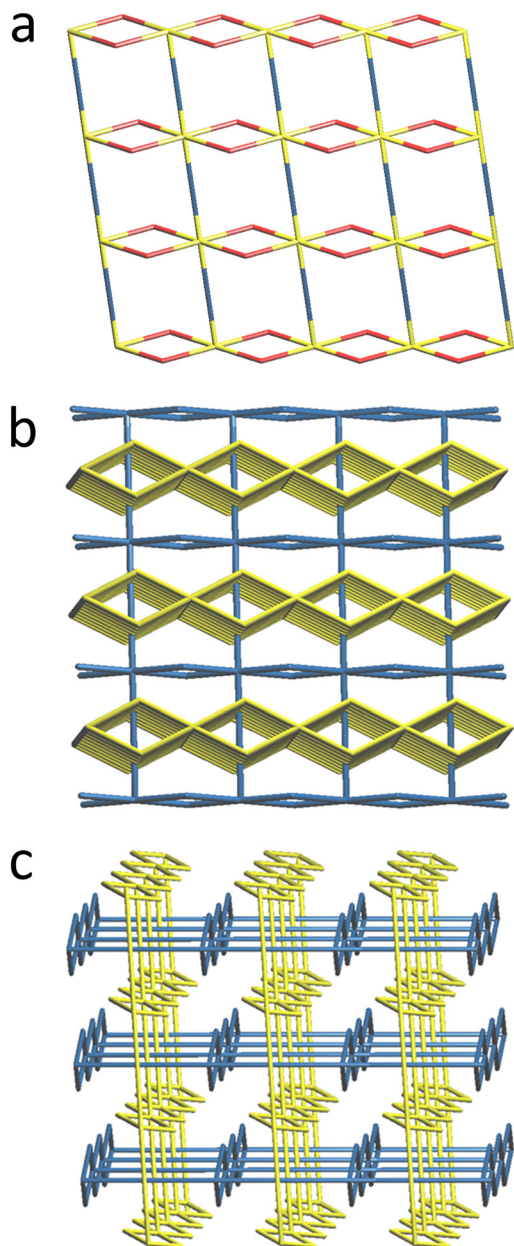


Fig. 5 (a) Nodal representation of the diperiodic network in **4** (yellow, tetranuclear U_4O_2 nodes; red, $kpim^{2-}$ edges; blue, $bcpcb$ edges). (b) Simplified representation of the crossing of the two families of layers. (c) Simplified representation of the polycatenated framework.

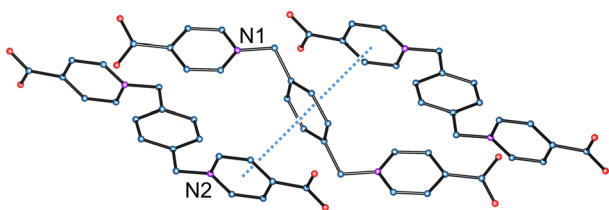


Fig. 6 π -Stacking interactions (dotted line) between $bcpcb$ molecules at the crossing point between polycatenated networks in **4**.

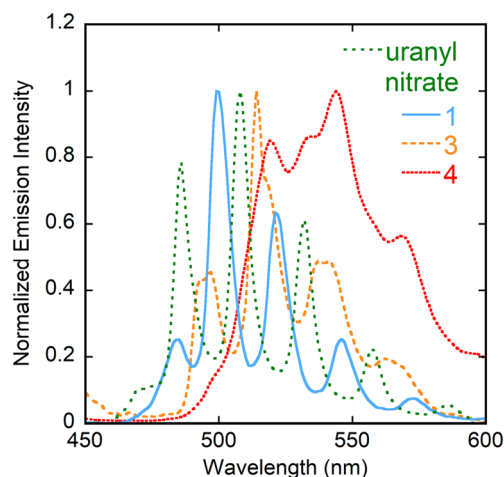


Fig. 7 Emission spectra of complexes **1**, **3** and **4**, and uranyl nitrate hexahydrate in the crystalline state upon excitation at 420 nm.

are anomalously large values for a carboxylate tris-chelated uranyl species,²⁶ possibly due to the influence of the zwitterionic donors. With main maxima at 496, 514, 539 and 562 nm, the spectrum of **3** is typical of a uranyl ion complex with an O_5 equatorial environment, but all peaks are split into two close components, the origin of this being uncertain since the asymmetric unit in the crystal structure contains a unique uranyl centre. Finally, the spectrum of **4** displays a very broad emission line with only three well-defined maxima at 519, 544 and 568 nm, here also typical of an O_5 environment, but it obviously contains a mixture of two components, probably corresponding to the two crystallographically independent uranyl sites. The presence of the μ_3 -oxo bridges may also contribute to the large redshift seen for this compound, through inducing a weakening of the $U=O$ bonds greater than that due to carboxylates, with this effect being probably larger than that recently demonstrated for hydroxide donors.²⁷ The spectrum of $[UO_2(NO_3)_2(H_2O)_2] \cdot 4H_2O$, recorded under the same conditions, is also shown in Fig. 7 for comparison; its four main maxima are at 486, 508, 532 and 557 nm, and it is thus blue-shifted with respect to the spectra of **1**, **3** and **4**. As a note of caution regarding the interpretation of ambient temperature, solid state emission spectra, there is evidence in low-temperature measurements of considerably greater complexity than is seen otherwise²⁸ and there is strong theoretical evidence to support its interpretation as that more than one vibrational mode can contribute to the vibronic progressions considered typical of uranyl ion emission;²⁹ the simplicity of the spectrum of complex **1** may thus be deceptive.

Conclusions

The four uranyl ion complexes described here, which include mixed anionic and zwitterionic carboxylate ligands, illustrate the variety of interactions which can be found in



such species. The monocarboxylate betaine acts as a terminating ligand and $\text{UO}_2(\text{pda})(\text{bet})_2$ units are simple decorating groups on a monoperiodic $\text{UO}_2(\text{pda})$ polymer in complex **1**. A more complicated situation arises with the zwitterionic dicarboxylate bcebp in complex **2**, with separation of the two ligand types in different polymeric units, diperiodic with tcenm^{3-} and monoperiodic with bcebp, and the additional presence of diprotonated bcebpH_2^{2+} counterions hydrogen bonded at both ends to monoperiodic chains through four intervening diperiodic layers, giving rise to a hydrogen bonded heteropolycatenated assembly. Two genuine mixed-ligand species are obtained with the bcpmb dizwitterion and either pht^{2-} (**3**) or kpim^{2-} (**4**) coligands, an additional complication arising from the presence of μ_3 -oxo bridges giving U_4O_2 SBUs in the latter case. While **3** crystallizes as a simple diperiodic network with V_2O_5 topology, **4** is a novel example of $2\text{D} + 2\text{D} \rightarrow 3\text{D}$ inclined polycatenation, thus confirming the interest in such large zwitterionic dicarboxylates for the synthesis of entangled species.

Another interesting aspect of this work is to provide some new insight on the difference in coordination strength between anionic and zwitterionic carboxylates. While the range of U–O(anionic carboxylate) bond lengths in **1** encompasses that of the U–O(zwitterion carboxylate) bond lengths, the latter all lie towards the longer end of the former and on the true mixed-ligand centres U3 and U4, in particular, those of the former are slightly shorter than those of the latter, which could perhaps be interpreted as indicating a slight preference for the anionic donors. The bond valence parameters for anionic and zwitterionic donors in **1**, **2** and **4** confirm the slightly greater donor strength of the former, as well as their stronger effect on the strength of the axial bonds. These results would offer at least a partial explanation of the increasing frequency with which our efforts, including the present examples, to generate mixed-ligand complexes have resulted in crystal structures where anionic- and zwitterionic-carboxylate donors are present in separate components. It need not be considered disadvantageous and indeed adds a new theme to our simple initial objective of using polyanionic donors to increase the periodicity of coordination polymers obtained with polyzwitterionic donors. The present structures provide evidence that these two families of ligands do tend to differ in regard to bonding *via* chelation and further bridging, with differences possibly associated with the capacity of the cationic centres of the zwitterions to be involved in their particular interactions. As is evident in general for uranyl ion coordination polymer structures, hydrogen bonding can be an important influence, especially when it is in competition with the weak equatorial coordination interactions of the uranyl ion.

Conflicts of interest

There are no conflicts of interest to declare.

Acknowledgements

This work was supported by Iketani Science and Technology Foundation, and KAKENHI Grant-in-Aid for Early-Career Scientists JP22K14698 (S. K.).

References

- (a) P. Thuéry and J. Harrowfield, *Inorg. Chem.*, 2022, **61**, 9725; (b) P. Thuéry and J. Harrowfield, *Eur. J. Inorg. Chem.*, 2022, e202200011; (c) P. Thuéry and J. Harrowfield, *CrystEngComm*, 2021, **23**, 7305.
- (a) S. Kusumoto, Y. Atoini, S. Masuda, Y. Koide, J. Y. Kim, S. Hayami, Y. Kim, J. Harrowfield and P. Thuéry, *CrystEngComm*, 2022, **24**, 7833; (b) S. Kusumoto, Y. Atoini, S. Masuda, J. Y. Kim, S. Hayami, Y. Kim, J. Harrowfield and P. Thuéry, *Inorg. Chem.*, 2022, **61**, 15182; (c) S. Kusumoto, Y. Atoini, S. Masuda, Y. Koide, J. Y. Kim, S. Hayami, Y. Kim, J. Harrowfield and P. Thuéry, *Inorg. Chem.*, 2023, **62**, 3929; (d) S. Kusumoto, Y. Atoini, S. Masuda, Y. Koide, K. Chainok, Y. Kim, J. Harrowfield and P. Thuéry, *Inorg. Chem.*, 2023, **62**, 7803; (e) S. Kusumoto, Y. Atoini, Y. Koide, K. Chainok, S. Hayami, Y. Kim, J. Harrowfield and P. Thuéry, *Chem. Commun.*, 2023, **59**, 10004.
- X. M. Chen and T. C. W. Mak, *J. Crystallogr. Spectrosc. Res.*, 1993, **23**, 291.
- L. Baklouti and J. Harrowfield, *Dalton Trans.*, 2023, **52**, 7772.
- (a) P. Nockemann, R. Van Deun, B. Thijs, D. Huys, E. Vanecht, K. Van Hecke, L. Van Meervelt and K. Binnemans, *Inorg. Chem.*, 2010, **49**, 3351; (b) P. A. Smith and P. C. Burns, *CrystEngComm*, 2014, **16**, 7244; (c) P. A. Smith, T. L. Spano and P. C. Burns, *Z. Kristallogr.*, 2018, **233**, 507; (d) P. A. Smith and P. C. Burns, *Z. Anorg. Allg. Chem.*, 2019, **645**, 504.
- (a) C. R. Groom, I. J. Bruno, M. P. Lightfoot and S. C. Ward, *Acta Crystallogr., Sect. B: Struct. Sci., Cryst. Eng. Mater.*, 2016, **72**, 171; (b) R. Taylor and P. A. Wood, *Chem. Rev.*, 2019, **119**, 9427.
- (a) K. X. Wang and J. S. Chen, *Acc. Chem. Res.*, 2011, **44**, 531; (b) M. B. Andrews and C. L. Cahill, *Chem. Rev.*, 2013, **113**, 1121; (c) T. Loiseau, I. Mihalcea, N. Henry and C. Volkringer, *Coord. Chem. Rev.*, 2014, **266–267**, 69; (d) J. Su and J. S. Chen, *Struct. Bonding*, 2015, **163**, 265; (e) P. Thuéry and J. Harrowfield, *Dalton Trans.*, 2017, **46**, 13660; (f) K. Lv, S. Fichter, M. Gu, J. März and M. Schmidt, *Coord. Chem. Rev.*, 2021, **446**, 214011.
- APEX3, ver. 2019.1-0, Bruker AXS, Madison, WI, 2019.
- SAINT, ver. 8.40A, Bruker Nano, Madison, WI, 2019.
- (a) SADABS, ver. 2016/2, Bruker AXS, Madison, WI, 2016; (b) L. Krause, R. Herbst-Irmer, G. M. Sheldrick and D. Stalke, *J. Appl. Crystallogr.*, 2015, **48**, 3.
- G. M. Sheldrick, *Acta Crystallogr., Sect. A: Found. Adv.*, 2015, **71**, 3.
- G. M. Sheldrick, *Acta Crystallogr., Sect. C*, 2015, **71**, 3.
- C. B. Hübschle, G. M. Sheldrick and B. Dittrich, *J. Appl. Crystallogr.*, 2011, **44**, 1281.



- 14 A. L. Spek, *Acta Crystallogr., Sect. C: Struct. Chem.*, 2015, **71**, 9.
- 15 (a) M. N. Burnett and C. K. Johnson, *ORTEP*, Report ORNL-6895, Oak Ridge National Laboratory, TN, 1996; (b) L. J. Farrugia, *J. Appl. Crystallogr.*, 2012, **45**, 849.
- 16 K. Momma and F. Izumi, *J. Appl. Crystallogr.*, 2011, **44**, 1272.
- 17 V. A. Blatov, A. P. Shevchenko and D. M. Proserpio, *Cryst. Growth Des.*, 2014, **14**, 3576.
- 18 N. E. Brese and M. O'Keeffe, *Acta Crystallogr., Sect. B: Struct. Sci.*, 1991, **47**, 192.
- 19 A. L. Spek, *Acta Crystallogr., Sect. D: Biol. Crystallogr.*, 2009, **65**, 148.
- 20 P. Thuéry, Y. Atoini and J. Harrowfield, *CrystEngComm*, 2023, **25**, 3904.
- 21 (a) I. Mihalcea, N. Henry and T. Loiseau, *Cryst. Growth Des.*, 2011, **11**, 1940; (b) I. Mihalcea, C. Volkringer, N. Henry and T. Loiseau, *Inorg. Chem.*, 2012, **51**, 9610; (c) J. Olchowka, C. Falaise, C. Volkringer, N. Henry and T. Loiseau, *Chem. – Eur. J.*, 2013, **19**, 2012; (d) A. T. Kerr, S. A. Kumalah, K. T. Holman, R. J. Butcher and C. L. Cahill, *J. Inorg. Organomet. Polym. Mater.*, 2014, **24**, 128; (e) X. Gao, C. Wang, Z. F. Shi, J. Song, F. Y. Bai, J. X. Wang and Y. H. Xing, *Dalton Trans.*, 2015, **44**, 11562; (f) X. Gao, J. Song, L. X. Sun, Y. H. Xing, F. Y. Bai and Z. Shi, *New J. Chem.*, 2016, **40**, 6077; (g) W. Xu, Z. X. Si, M. Xie, L. X. Zhou and Y. Q. Zheng, *Cryst. Growth Des.*, 2017, **17**, 2147; (h) L. W. Zeng, K. Q. Hu, L. Mei, F. Z. Li, Z. W. Huang, S. W. An, Z. F. Chai and W. Q. Shi, *Inorg. Chem.*, 2019, **58**, 14075; (i) G. Andreev, N. Budantseva, A. Levitsova, M. Sokolova and A. Fedoseev, *CrystEngComm*, 2020, **22**, 8394; (j) P. Thuéry and J. Harrowfield, *Cryst. Growth Des.*, 2021, **21**, 3000.
- 22 L. Mei, Z. N. Xie, K. Q. Hu, L. Y. Yuan, Z. Q. Gao, Z. F. Chai and W. Q. Shi, *Chem. – Eur. J.*, 2017, **23**, 13995.
- 23 (a) S. W. An, L. Mei, K. Q. Hu, C. Q. Xia, Z. F. Chai and W. Q. Shi, *Chem. Commun.*, 2016, **52**, 1641; (b) S. W. An, L. Mei, K. Q. Hu, F. Z. Li, C. Q. Xia, Z. F. Chai and W. Q. Shi, *Inorg. Chem.*, 2019, **58**, 6934; (c) M. L. Brown and D. B. Leznoff, *Can. J. Chem.*, 2020, **98**, 365.
- 24 (a) M. S. Grigoriev, C. Den Auwer, P. Meyer and P. Moisy, *Acta Crystallogr., Sect. C: Cryst. Struct. Commun.*, 2006, **62**, m163; (b) P. Thuéry, *Inorg. Chem. Commun.*, 2007, **10**, 423; (c) P. Thuéry, *CrystEngComm*, 2008, **10**, 808; (d) Z. Wang, X. Hou and S. F. Tang, *J. Coord. Chem.*, 2021, **74**, 1693.
- 25 (a) A. Brachmann, G. Geipel, G. Bernhard and H. Nitsche, *Radichim. Acta*, 2002, **90**, 147; (b) M. Demnitz, S. Hilpmann, H. Lösch, F. Bok, R. Steudtner, M. Patzschke, T. Stumpf and N. Huittinen, *Dalton Trans.*, 2020, **49**, 7109.
- 26 P. Thuéry and J. Harrowfield, *Inorg. Chem.*, 2017, **56**, 13464.
- 27 Y. H. Dai, Z. Zhao, Z. X. Wang, N. Liu, F. Z. Li and J. Su, *Eur. J. Inorg. Chem.*, 2023, e202300090.
- 28 R. G. Surbella, M. B. Andrews and C. L. Cahill, *J. Solid State Chem.*, 2016, **236**, 257.
- 29 H. Oher, F. Réal, T. Vercoouter and V. Vallet, *Inorg. Chem.*, 2020, **59**, 5896.

